

The spatio-temporal variations of frost-free period in China from 1951 to 2012

NING Xiaoju^{1,2}, LIU Gangjun³, ZHANG Lijun¹, QIN Xiaoyang⁴, ZHOU Shenghui¹,
*QIN Yaochen^{1,2}

1. College of Environment and Planning, Key Laboratory of Geospatial Technology for Middle and Lower Yellow River Regions, Henan University, Kaifeng 475004, Henan, China;
2. College of Resources and Environment, Henan Three New-Types Coordinated Development Center, Henan University of Economics and Law, Zhengzhou 450046, China;
3. College of Science, Engineering and Health, RMIT University, 124 LaTrobe Street, Melbourne 3000, Australia;
4. Institute of Geography, Henan Academy of Sciences, Zhengzhou 450052, China

Abstract: The frost-free period (FFP), first frost date (FFD) and last frost date (LFD) have been regarded as the important climate variables for agricultural production. Understanding the spatio-temporal variations of the FFP, FFD and LFD is beneficial to reduce the harmful impacts of climate change on agricultural production and enhance the agricultural adaptation. This study examined daily minimum temperatures for 823 national-level meteorological stations, calculated the values of FFD, LFD and FFP for station-specific and region-specific from 1951 to 2012, estimated the gradients of linear regression for station-specific moving averages of FFD, LFD and FFP, and assessed station-specific time series of FFP and detected the abrupt change. The results as follows: at both the station level and the regional level, the FFP across China decreases with the increase of latitude from south to north, and with the increase of altitude from east to west generally. At the station level, the inter-annual fluctuations of FFD, LFD and FFP in south and west agricultural regions are greater than those in north and east. At the regional level, excluding the QT region, temporal changes of FFP are relatively small in both the low-latitude and the high-latitude regions, but for the mid-latitude regions. According to the linear trend gradients of the moving average values of station-specific FFD, LFD and FFP, FFD was delayed, LFD advanced, and FFP extended gradually over the 80% of China. Furthermore, the change magnitudes for FFD, LFD and FFP in the north and east agricultural regions are higher than that in the southern and western. Among the 659 station-specific time series of FFP examined by the Mann-Kendall test, 341 stations, located mainly in the north region, have one identifiable and significant abrupt change. And at the 341 stations with identified abrupt changes, most (57%) abrupt changes occurred during 1991–2012, followed by the periods of 1981–1990 (28%), 1971–1980 (12%), and 1951–1970 (3%). The spatio-temporal variations of FFD, LFD and FFP would provide

Received: 2016-07-06 **Accepted:** 2016-08-30

Foundation: National Basic Program of China (973 Program), No.2012CB955800; National Natural Science Foundation of China, No.41671536, No. 41501588; Qinghai Key Laboratory Open Fund of Disaster Prevention and Reduction, No.QHKF201401; Key Scientific Research Projects in Colleges and Universities, No.17A170005

Author: Ning Xiaoju (1987–), specialized in sustainable development. E-mail: nxj0655@163.com

***Corresponding author:** Qin Yaochen (1959–), Professor, specialized in a regional model on sustainable development and geographic information science. E-mail: qinye@henu.edu.cn

important guidance to agricultural practices.

Keywords: frost-free period; first frost date; last frost date; spatio-temporal variations; agricultural region; China

1 Introduction

Global warming increases the heat stress of crops and hence influences the crop yields (IPCC, 2014; Edmar *et al.*, 2013; Ramirez-Villegas *et al.*, 2013). The frost-free period (FFP), and the related first frost date (FFD) and last frost date (LFD), are important indicators of temperature variations (Li *et al.*, 1988). We could reduce the negative impacts of extreme low temperature events on agriculture production, and select the suitable crop types and adjust the crop systems to enhance the agricultural adaptation to climate change by analyzing the spatio-temporal variation in FFP, FFD and LFD (Han *et al.*, 2010; Zhang *et al.*, 2014). Therefore, there have been a great number of literatures highlighting the FFP and the related FFD and LFD (Qian *et al.*, 2012; Skaggs and Irmak, 2012).

On the onset of FFD, Han *et al.* (2010) revealed a clear later FFD in northern China since 2000. The FFD was delayed significantly in Shanxi province between 1970 and 2009, with an abrupt change occurring in 2000 (Qian *et al.*, 2010). The similar delayed trend of FFD was observed in the neighboring Shaanxi province, with an average delaying for 1.4 days per 10 years (Bai *et al.*, 2013). FFD was delayed for about 11 days between 1960 and 2011 in the Xinjiang region (Pan *et al.*, 2013), with the delayed rate of 2.21 days per 10 years (Zhang *et al.*, 2013). Under the influence of climate warming, the delayed rate of FFD in northwest China was 1.8 days per decade, and FFD witnessed the abrupt change in 1986 (Chen *et al.*, 2013; Li and Shen, 2013). In the last five decades, records from some stations in the Tibet region on the FFD also showed a delaying trend (Du *et al.*, 2013). The delayed rate for the FFD in the Hengduan Mountains was about 1.09 days per decade (Wang *et al.*, 2014). Even for the Chongqing region located in the south, the FFD also displayed a delaying trend during the last four decades (Du *et al.*, 2014).

With regards to the arrival of LFD, the LFD of Shanxi province fluctuated on the dominant temporal variation, with multiple abrupt changes occurring between 1975 and 1996. However, the spatial differentiation of LFD was obvious in Shanxi province. There was a much earlier LFD in the central-western and southern parts, contrasted by the much later LFD in the central-eastern and northwestern parts (Li *et al.*, 2013). In average, the LFD has advanced for about 1.7 days per decade in Shaanxi province (Bai *et al.*, 2013), and for about 1.41 days per decade from 1960 to 2011 in the Xinjiang region (Pan *et al.*, 2013; Zhang *et al.*, 2013). The LFD has also advanced significantly in the north China and the Hengduan Mountains from 1963 to 2009 and from 1990 to 1999, respectively (Dai *et al.*, 2013; Wang *et al.*, 2014). However, the LFD in the Chongqing region was delayed (Du *et al.*, 2014).

Influenced by changes in both the FFD and LFD, the FFP also varied. Researchers have revealed that the FFP has increased in some areas, such as northwest China, Shanxi province, Shaanxi province, and Hengduan Mountains, due to the combined effects of a later FFD and an earlier LFD (Qian *et al.*, 2010; Bai *et al.*, 2013; Pan *et al.*, 2013; Zhang *et al.*, 2013; Li and Shen, 2013; Wang *et al.*, 2014). The slow increase of FFP in the Chongqing region was due to the combined effects of much delayed FFD and slightly delayed LFD (Du *et al.*,

2014). With readily available FFP observations, some researchers did not relate the changes in FFP with the timing of FFD and LFD, but focused on the trends of change in FFP. For instance, Zhang *et al.* (2013) found that the rate of increase in FFP in the Ningxia region was about 4.7 days per decade between 1961 and 2010, with an abrupt change occurring in 1982. The rate of increase in FFP was about 3.5 days per decade in northeast China, with the contour line of FFP towards the north (Hu *et al.*, 2015). In the Tibet region, changes in the number of frost days have been used as a proxy for characterizing changes in FFP. The number of frost days has decreased in the Tibet region, but the decreased range varied in different parts of Tibet (Labaciren *et al.*, 2014). Through the frost days forecasted by the R/S method, Du *et al.* (2013) hinted that the FFP would increase in many parts of the Tibet region gradually in future.

However, researches on FFD, LFD, FFP and its abrupt changes, as well as the inter-relationships among these agro-climate variables by now, only covered limited areas, concerned inconsistent time periods, and have not yet established a clear understanding of the characteristics of spatio-temporal variations of FFP across China. This study aims at, first, establishing a general understanding of the characteristics of spatio-temporal variations of FFP across China between 1951 and 2012, in terms of estimated regional averages of FFD, LFD and FFP based on the 9 agricultural regions of China (NAZC, 1981); and then, through spatial interpolation of station-based calculation of FFD, LFD and FFP, to reveal China-wide spatial distributions of FFD, LFD and FFP, estimate their linear trends and inter-relationships, and examine when and where abrupt changes in FFP occurred.

2 Data and method

2.1 Data

Both time series of daily minimum temperature between 1951 and 2012 and location data for national-level meteorological stations are obtained for this study from the Chinese meteorological data hub (<http://www.escience.gov.cn/metdata/page/index.html>). In China, there are only 152 national-level meteorological stations in 1951; the number increased rapidly to 766 in 1960; and 824 stations are in operation till 2012. Among the 824 stations, one station takes records only in certain seasons, and 97 stations are located in the southern agricultural regions that recorded only a few frost days between 1951 and 2012. Therefore, time series of daily minimum temperature between 1951 and 2012 from only 726 stations can be used for the determination of FFD, LFD and FFP. At the 726 stations, 67 stations missing records in some years, and only 659 stations' data are usable for the Mann-Kendall test for detecting abrupt changes in time series. Boundary of the 9 agricultural regions in China is downloaded from National Earth System Science Data Sharing Information (<http://www2.geodata.cn/index.html>) in shape file format. The types of spatial distribution for the 9 agricultural regions in China are shown in Figure 1.

2.2 Method

The characteristic spatio-temporal variations in FFD, LFD, and FFP across China between 1951 and 2012 are derived via the following procedures (Figure 2): calculate station-specific values of FFD, LFD, and FFP; compute region-specific values of FFD, LFD, and FFP; esti-

mate linear trends of station-specific values of FFD, LFD, and FFP; and detect abrupt changes in station-specific time series of FFP.

2.2.1 Calculate the station-specific values of FFD, LFD and FFP

Generally, both FFD and LFD are calculated with measured ground temperatures (Han *et al.*, 2010). However, due to limited availability of measured ground temperatures, daily minimum temperatures (DMT) are usually used to calculate the FFD and LFD. In this study, the DMT data, which obtained from the meteorological stations, are adopted to calculate station-specific FFD, LFD and FFP. Then convert the FFD, LFD and FFP to Julian calendar for analyzing their temporal changes and trends.

For each of the 823 stations, year-specific dates of FFD_{ij} , LFD_{ij} , the corresponding FFP_{ij} , and their means (μFFD_i , μLFD_i , μFFP_i) and standard deviations (σFFD_i , σLFD_i , σFFP_i) between 1951 and 2012 are obtained, where i ($= 1 \dots 823$) refers to stations and j ($= 1 \dots 62$) refers to years. For most stations, mainly in the northern parts of China, FFD_{ij} is specified as the first time since autumn when daily minimum temperature observed at the station (DMT_{ij}) is equal to or below 0°C , LFD_{ij} is specified as the last time before summer when DMT_{ij} is equal to or below 0°C , and FFP_{ij} is specified as the total number of days fall between LFD_{ij} and FFD_{ij} . For some stations, mainly in

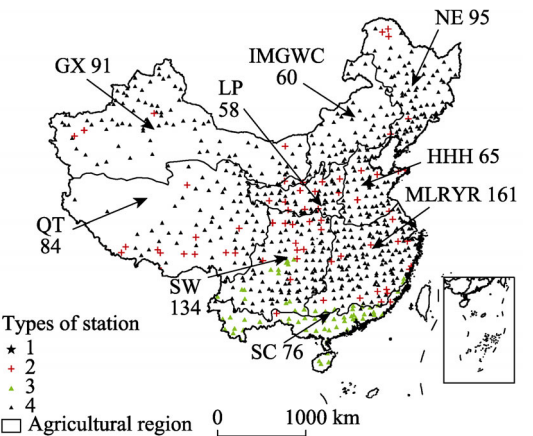


Figure 1 The 9 agricultural regions and 824 national-level meteorological stations used in the study
Notes: I. Station types: 1. The station with records only in certain seasons; 2. The 67 stations with missing records for some years; 3. The 97 stations recorded frost-free period longer than 360 days; 4. The 659 stations with records of frost periods that are usable for the Mann-Kendall test. II. Agricultural regions: Gansu-Xinjiang (GX) region, Inner Mongolia and Great Wall Corridor (IMGWC) region, Northeast (NE) region, Huang-Huai-Hai (HHH) region, Loess Plateau (LP) region, Southwest (SW) region, South China (SC) region, Mid-and-Lower Reaches of the Yangtze River (MLRYR) region, Qinghai-Tibet (QT) region. III. The northern agricultural regions include IMGWC, NE, HHH, and LP regions; while the southern agricultural regions include SW, SC, and MLRYR.

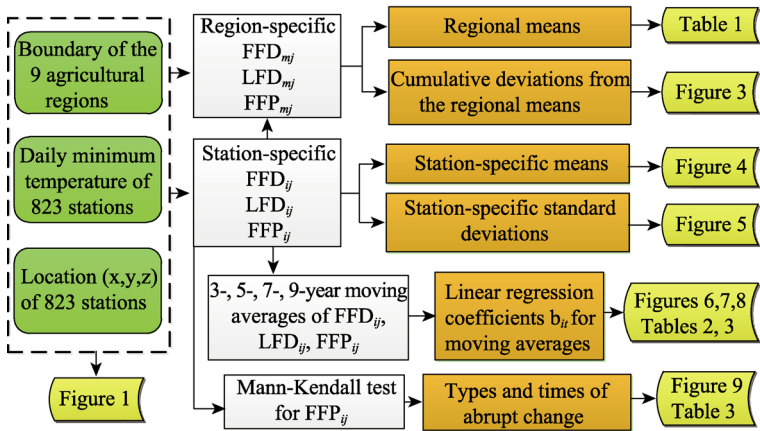


Figure 2 The methodology applied in this study

the southern parts of China, where the records indicate no dates when DMT_{ij} is equal to or below 0°C , both FFD_{ij} and LFD_{ij} are set to null, and FFP_{ij} is set to 365 days for non-leap years, and 366 for leap years.

Universal kriging is regarded as a useful and data-driven spatial interpolation method for transforming a point-based representation of climate variables into climate surfaces or fields (Tang and Yang, 2012). This study transforms the 823 point-base values into a set of raster surfaces by the universal kriging, and characterise the spatial variations of FFD, LFD and FFP.

2.2.2 Compute region-specific values of FFD, LFD and FFP

Cumulative deviation from the mean (CDFM) is a commonly used technique for detecting trends in time series (Wei, 2007). In this study, the cumulative annual deviations from the regional averages of FFD, LFD and FFP are derived to illustrate their region-specific trends of temporal variations. Based on the spatial overlay and statistical summary, the cumulative annual deviations from the regional average for each of the 9 agricultural regions are derived through three steps:

First, select all stations within each region, and calculate the 9×62 annual regional averages for FFD, LFD and FFP (μFFD_{mj} , μLFD_{mj} , μFFP_{mj}) and the 9 regional averages over the 62 years (μFFD_m , μLFD_m , μFFP_m), where m ($= 1 \dots 9$) refers to specific region and j ($= 1 \dots 62$) specific year. The regional averages are summarised in Table 1.

Second, calculate the 9×62 annual deviations from the regional averages ($\Delta FFD_{mj} = \mu FFD_{mj} - \mu FFD_m$, $\Delta LFD_{mj} = \mu LFD_{mj} - \mu LFD_m$, $\Delta FFP_{mj} = \mu FFP_{mj} - \mu FFP_m$).

Third, calculate the 9×61 cumulative annual deviations from the regional average ($\Sigma \Delta FFD_{mj}$, $\Sigma \Delta LFD_{mj}$, $\Sigma \Delta FFP_{mj}$) in a manner of $\Sigma \Delta FFD_{mj+2} = \Sigma \Delta FFD_{mj} + \Sigma \Delta FFD_{mj+1}$, $\Sigma \Delta LFD_{mj+2} = \Sigma \Delta LFD_{mj} + \Sigma \Delta LFD_{mj+1}$, and $\Sigma \Delta FFP_{mj+2} = \Sigma \Delta FFP_{mj} + \Sigma \Delta FFP_{mj+1}$, and to illustrate the general trends of temporal variations of FFD, LFD and FFP for each region, by plotting $\Sigma \Delta FFD_{mj}$, $\Sigma \Delta LFD_{mj}$ and $\Sigma \Delta FFP_{mj}$ on the y-axis against the year on the x-axis (Figure 3).

2.2.3 Estimate linear trends of station-specific values of FFD, LFD and FFP

Linear trend estimate is regarded as useful for indicating trends and rates of changes in time series of climate variables (Wei, 2007). In this study, moving averages of station-specific time series of FFD, LFD and FFP are used to build linear trend models and, based upon these models, to examine their trends and rates of changes between 1951 and 2012. This task also involves three steps:

First, calculate 3-, 5-, 7-, and 9-year moving averages of FFD_{ij} , LFD_{ij} and FFP_{ij} (FFD_{it} , LFD_{it} or FFP_{it} , where $t = 3, 5, 7, 9$).

Second, determine station-specific linear regression coefficients b_{it} (as in $y_{it} = a_i + b_{it}x_{it}$, where $x_{it} = FFD_{it}$, LFD_{it} or FFP_{it} , and y_{it} are best linearly fitted values of FFD_{it} , LFD_{it} or FFP_{it} , and use b_{it} as a proxy for the linear trend gradient of temporal variations in FFD_{it} , LFD_{it} , and FFP_{it}).

Third, characterise the spatial variations of station-specific linear trends of FFD, LFD and FFP, by transforming the 823 point-based values of b_{it} into a set of raster surfaces (Figures 6–8), and summarising area percentage associated with b_{it} for FFD_{it} , LFD_{it} and FFP_{it} (Tables 2 and 3).

2.2.4 Detect abrupt changes in station-specific time series of FFP

The Mann-Kendall test (Mann, 1945; Kendall, 1967; Goossens and Berger, 1986) is a non-parametric (distribution-free) test that can be used in place of a parametric linear regression analysis to test if the slope of the estimated linear regression line is different from zero. The Mann-Kendall test is often used to statistically assess if there is a monotonic, linear or non-linear, upward or downward trend of the variable of interest over time, or detect if and when abrupt changes happen in time series from one monotonic upward (downward) trend to another (Fu and Wang, 1992). In this study, the Mann-Kendall test is used to detect abrupt changes in station-specific time series of FFP across China, and is implemented in the Matlab environment as follows:

- (1) Let x_{ij} denote FFP_{*ij*}, the FFP value at station *i* for year *j*, and for each station *i*, order x_{ij} over time, $x_{i1}, x_{i2}, \dots, x_{in}$.
- (2) Find all $n(n-1)/2$ possible differences $r_{ik} = x_{ik} - x_{il}$, where $k > l$, $k=2, \dots, n$, $l=1, 2, 3, \dots, k$, including $x_{i2}-x_{i1}, x_{i3}-x_{i1}, \dots, x_{in}-x_{i1}, x_{i3}-x_{i2}, x_{i4}-x_{i2}, \dots, x_{in}-x_{in-2}, x_{in}-x_{in-1}$.
- (3) Let $r_{ik} = 1$, if $x_{ik}-x_{il} > 0$, means that the value of *x* at time *k* is greater than that at time *l*; and $r_{ik} = 0$, if $x_{ik}-x_{il} \leq 0$, means that the value of *x* at time *k* is less than that at time *l*.
- (4) Compute S_{ik} as follows:
$$S_{ik} = \sum_{k=2}^n \sum_{l=1}^k r_{ik}.$$
- (5) For each S_{ik} , compute its expected value, $E(S_{ik}) = k(k-1)/4$, variance, $V(S_{ik}) = k(k-1)(2k+5)/72$, and UF_{ik} value, $UF_{ik} = \frac{S_{ik} - E(S_{ik})}{\sqrt{Var(S_{ik})}}$.
- (6) Reverse the order of x_{ij} over time, $x_{in}, x_{in-1}, x_{in-2}, \dots, x_{i1}$, and then compute the UB_{ik} in the same manner as described in steps 2–5 above.
- (7) Plot the UF_{ik} and UB_{ik} curves, detect the abrupt changes (or intersection points, if any), and classify the 659 qualified stations into three types (Figure 9 and Table 4):
 - a) for type 1 stations, the UF_{ik} and UB_{ik} curves have only one intersect point which lies within the confidence region ($u_{\alpha=0.05}=\pm 1.96$);
 - b) for type 2 stations, the UF_{ik} and UB_{ik} curves also have only one intersect point but lies outside the confidence region ($u_{\alpha=0.05}=\pm 1.96$);
 - c) for type 3 stations, the UF_{ik} and UB_{ik} curves have more than two intersect points.
- (8) Identify time of abrupt changes in FFP that are associated only with type 1 station UF_{ik} and UB_{ik} curves.

3 Results and analysis

3.1 Evolving spatial distributions of FFD, LFD and FFP in agricultural regions

Regional average values of FFD, LFD and FFP determined for the 9 agricultural regions in China are summarised in Table 1. It is clear that the QT region has the shortest frost-free period, the earliest onset of FFD, and the latest arrival of LFD. As for the NE and IMGWC regions, they have similar lengths of frost-free period and similar dates for both FFD and LFD. Compared with the IMGWC region, the onset of FFD in the GX region is about one week later, the arrival of LFD is about two weeks earlier, and consequently, the frost-free

period is about 20 days longer. Compared with the GX region, the onset of FFD in the LP region is about two weeks later, the arrival of LFD is about one week earlier, and consequently, the frost-free period is about 20 days longer. Located toward the east of the LP region, with a lower altitude, and closer to the sea, the HHH region has a much later onset of FFD, a much earlier LFD, and consequently, a longer frost-free period. Compared with the northern agricultural regions (of NE, IMGWC, GX, LP, HHH), the southern agricultural regions (of MLRYR, SW) exhibit greater variations in FFD, LFD and FFP: the FFD varies orderly from November in the north, through December in the middle, to January next year in the south, corresponding changes are shown for the LFD, and the FFP varies between 200 and 365 days, with an average about 300 days. In the SC region, no stable dates of FFD and LFD exist, and the FFP covers almost the whole year.

Table 1 Regional averages for FFD, LFD and FFP determined for the 9 agricultural regions in China

Region-ID (m)	Region code	μFFD_m (date)	μLFD_m (date)	μFFP_m (days)
1	QT	18 September	27 May	116
2	NE	3 October	3 May	154
3	IMGWC	1 October	2 May	152
4	GX	9 October	19 April	173
5	LP	22 October	13 April	192
6	HHH	10 November	26 March	229
7	MLRYR	Uncertain	Uncertain	295
8	SW	Uncertain	Uncertain	300
9	SC	Uncertain	Uncertain	363

The temporal variations in FFD, LFD and FFP throughout the 62 years, within each of the nine agricultural regions, are characterised by means of the CDFM curves (Figure 3). In the QT region, the CDFM curve for FFD (i.e. the red curve in Figure 3a) indicates three phases: (1) a short initial increasing phase until the mid-1950s, indicating the FFD is gradually postponed; (2) a long, continuous decreasing phase until about 1990, indicating the FFD is shifted continuously to an earlier date; and (3) another increasing phase since about 1990, indicating FFD is again postponed gradually. Temporal variation in LFD in the QT region shifted gradually to an earlier date until the mid-1950s, then postponed continuously until about 1990, and again shifted gradually to an earlier date since around 1990 (i.e. the blue curve in Figure 3a). Consequently, FFP in the QT region increased gradually until the mid-1950s, then decreased continuously until about 1990, and again increased gradually since the early 1990s (i.e. the green curve in Figure 3a).

The temporal variations in the onset of FFD for both GX and NE regions (i.e. the red curves in Figures 3b and 3c), are as follows: the arrival of LFD in both regions are postponed continuously until the mid- to late-1980s; then, shifted gradually to an earlier date; and consequently, the temporal variation in FFP (i.e. the green curves in Figures 3b and 3c), exhibits fluctuating patterns similar to the temporal variations in FFD.

For both IMGWC and LP regions, the onset of FFD shifted gradually to an earlier date until the mid-to-late 1980s, then postponed continuously since the 1980s (i.e. the red curves

in Figures 3d and 3e). The arrival of LFD is postponed gradually until the mid-to-late 1980s, and then shifted continuously to an earlier date since the 1990s (i.e. the blue curves in Figures 3d and 3e). Consequently, FFP decreased gradually until the mid-to-late 1980s, and since then, increased continuously, as indicated by the CDFM curves for FFP (i.e. the green curves in Figures 3d and 3e).

In the HHH region, the onset of FFD postponed gradually until the early 1970s, then shifted continuously to an earlier date (i.e. the red curve in Figure 3f); the arrival of LFD postponed gradually until the mid-to-late 1980s, then shifted to an earlier date (i.e. the blue curve in Figure 3f). Consequently, FFP in the HHH region decreased gradually until the early 1990s and then increased continuously (i.e. the green curve in Figure 3f).

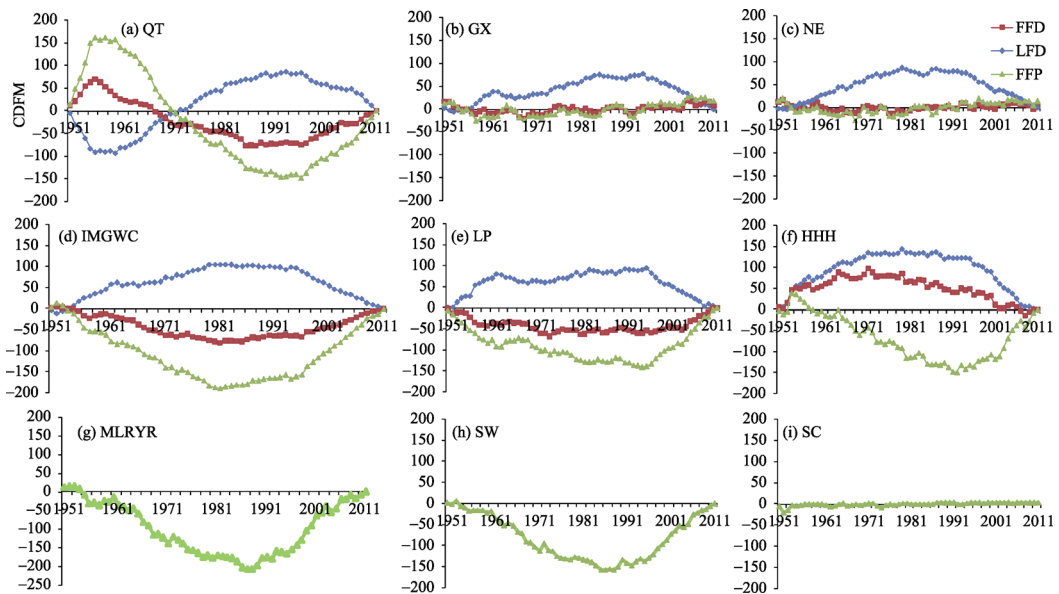


Figure 3 CDFM curves indicating temporal variations in FFD (red), LFD (blue) and FFP (green) in the 9 agricultural regions in China

For the MLRYR, SW and SC regions, temporal variation is characterised only for FFP (Figures 3g, 3h and 3i), due to unstable dates of FFD onset and LFD arrival. In the SC region, the temporal variation in FFP is not obvious, since the frost-free period covers almost the whole year. In both MLRYR and SW regions, FFP decreased gradually until the mid-to-late 1980s, and then increased continuously, with more pronounced changes shown in the MLRYR region.

3.2 Spatial variations of FFD, LFD and FFP across China

The spatial variation of FFP across China and its changes with time are shown in Figure 4, including the spatial variations in the FFP for 1960 (Figure 4a), 1970 (Figure 4b), 1980 (Figure 4c), 1990 (Figure 4d) and 2000 (Figure 4e), and the average of FFP (μ FFP) between 1951 and 2012 (Figure 4f). It is clear that the FFP decreases from south to north as latitude increases, and decreases from east to west as altitude increases. The μ FFP is over 300 days across the SC region, most parts of the SW region and the southern MLRYR region, and

reduced to about 250–300 days for the northern MLRYR region and part of the SW region. The contour line of μ FFP = 200 days stretches from the NE to the SW across China: from the northern HHH region, across the LP and SW regions, to the southeastern edge of the QT region, where the contours of μ FFP change rapidly. The μ FFP for most part of the QT region is under 100 days. Many parts of the QT region, in fact, have permafrost and daily average temperatures as low as 0°C in most part of the year, leading to none or only a few frost-free days. The μ FFP for the GX region ranges from about 150 days in the north, due to higher latitude and altitude and lower temperature resulted from the orographic effect of the Tian-shan Mountains. The contour line of μ FFP = 150 days basically delineates the IMGWC and the NE region into two parts: the μ FFP is less than 150 days in the north, due to higher latitude and altitude, and the μ FFP is about 150–200 days in the south, due to lower latitude and altitude.

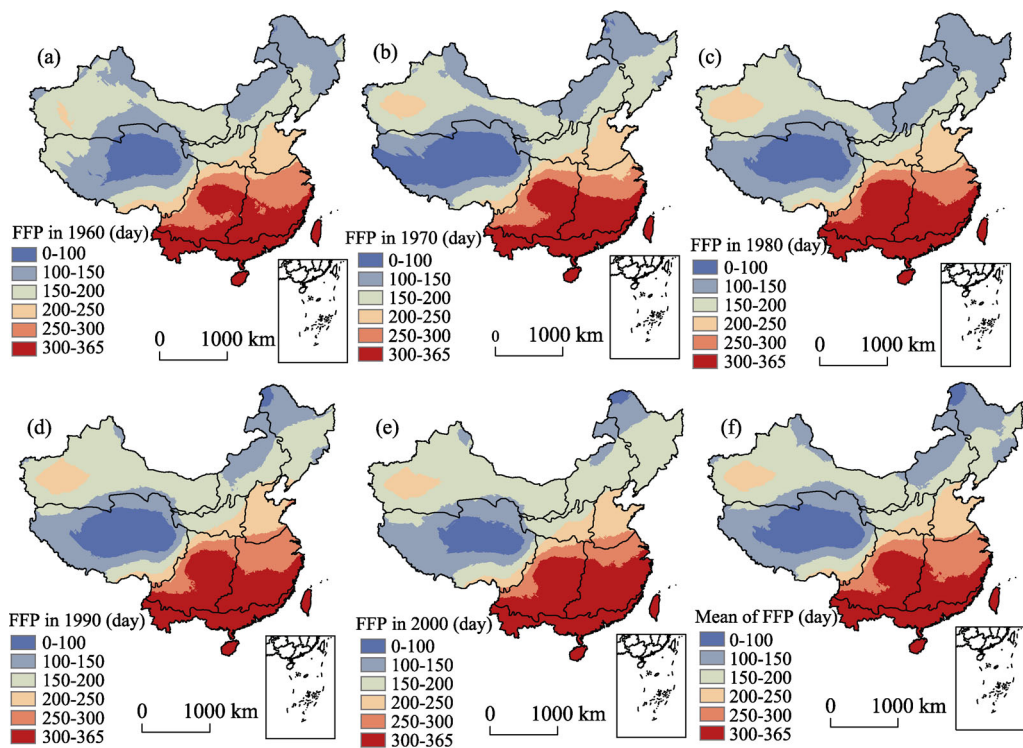


Figure 4 Spatial distributions of FFP in 1960 (a), 1970 (b), 1980 (c), 1990 (d), 2000 (e), and mean FFP (f)

Changes in the spatial distribution of FFP across China through time are revealed through changes in the contours of FFP in the five annual maps (Figures 4a–4e). The annual maps show that the contour line of FFP = 300 days shifted gradually towards the north between 1960 and 1980, and that the area with FFP >300 days expanded noticeably. This trend reversed in 1990. But since 2000, the contour line of FFP = 300 days shifted continuously northward again, resulted in the largest extent of area with FFP >300 days in 2000. In the QT region, the area with FFP <100 days expanded between 1960 and 1970, and then contracted from 1980 to 2000. For the IMGWC and NE regions, noticeable changes are shown for areas bounded by contours of FFP = 100 days and FFP = 150 days: the areas contracted in 1970 then expanded markedly and occupied over 80% of the two regions in 1980, and contracted

again rapidly and sequentially in 1990 and 2000.

The spatial distributions in the magnitudes of inter-annual changes in FFD, LFD and FFP are shown by means of the thematic maps of σ FFD (Figure 5a), σ LFD (Figure 5b), and σ FFP (Figure 5c), interpolated from their respective station-based values using universal kriging to take local trends into account.

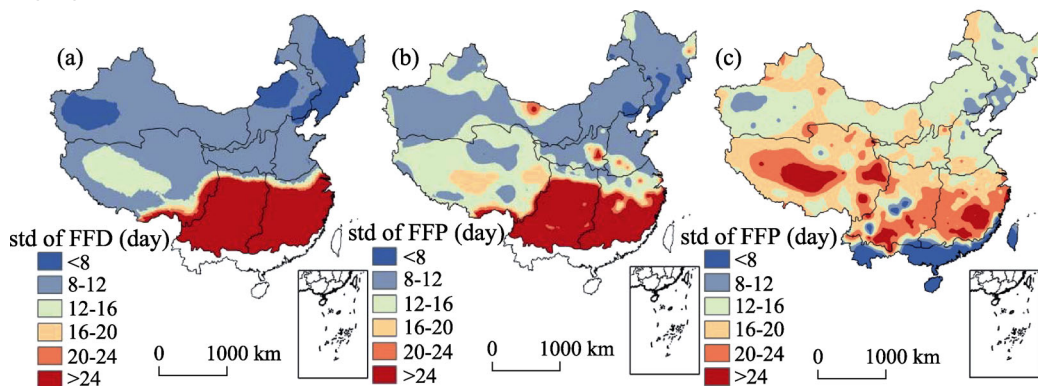


Figure 5 Spatial distributions of the standard deviations of the FFD (a), LFD (b) and FFP (c)

Figures 5a and 5b show that, in general, both σ FFD and σ LFD decrease from south to north, as latitude increases, and increase from east to west as altitude increases. The spatial distribution of σ LFD is more fragmented than that of σ FFD. In terms of the dates of FFD and LFD, the northern agricultural regions have more stability while the southern agricultural regions have larger magnitudes of fluctuations, because the southern regions are influenced more by changes in the strength or intensity of the southward moving cold air mass during winters. Most areas have greater stabilities in the date of FFD but greater fluctuations in the date of LFD. The SC region has no values for both σ FFD and σ LFD, due to the fact that few FFD and LFD records are found at stations in the region.

Figure 5c shows that, in general, σ FFP increases with altitude from east to west. With the increase in latitude northward, σ FFP shows a general trend of increase in the QT, SW and MLRYR regions, followed by a general trend of decrease in the northern agricultural regions. However, low σ FFP are clearly observable in relatively low-lying plains and basins across China. Higher values of σ FFP are observed in the QT, SW and MLRYR regions, while the SC region has the lowest σ FFP value. These results indicate strong influence of topography on the spatial distributions in the magnitudes of inter-annual changes in FFP, and confirm in principle the findings of Ye and Zhang (2008). The numerical results presented here do not compare exactly in values with previous findings, due to different datasets used. For example, Ye and Zhang (2008) used a dataset covering the 1961–2007 period, but this study uses a dataset covering a longer period between 1951 and 2012.

3.3 Temporal variations in FFD, LFD and FFP across China

3.3.1 Linear trends of changes in FFD, LFD and FFP

The general trends in the spatio-temporal variations in FFD, LFD and FFP from 1951 to 2012 across China, are represented with a set of thematic maps, displaying surfaces of linear

trend gradients b_t ($t = 3, 5, 7, 9$) of FFD (Figure 6), LFD (Figure 7) and FFP (Figure 8). These surfaces are interpolated from station-based values using the universal kriging technique. No linear trend gradients b_t of FFD, LFD and FFP are estimated for stations in the SC region because few FFD and LFD events have been recorded for most part of the region.

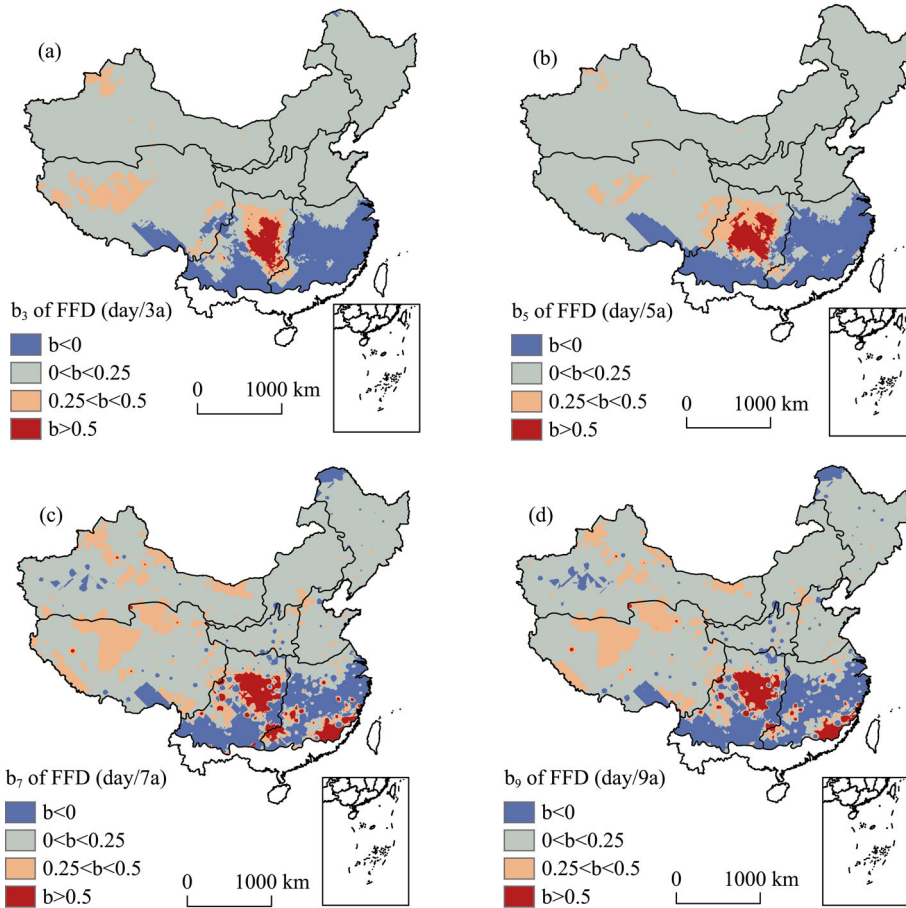


Figure 6 Surfaces of linear trend gradients b_t in FFD for the 3-, 5-, 7-, and 9-year moving averages (a, b, c, d)

Figure 6 shows that the linear trend gradients b_t for FFD increase as latitude increases from south to north. The linear trend gradients b_t for FFD are shown as positives in most parts of the agricultural regions and as negatives only in the SW and MLRYR regions, indicating a general trend of postponing in the onset of FFD for most part of China from 1951 to 2012. The linear trend gradients b_t for FFD fall between 0 and 0.25 for over 70% of China most of the times. Areas associated with linear trend gradients of $0 < b_t < 0.25$ expand to the largest extent on the 5-year moving average surface (i.e. the b_5 surface of FFD), and become relatively fragmented on the b_7 and b_9 surfaces of FFD, due to the emergence of larger patches associated with linear trend gradients of $0.25 < b_t < 0.5$ and smaller patches associated with negative linear trend gradients of $b_t < 0$ on these surfaces. Areas associated with higher linear trend gradients of $b_t > 0.5$ concentrate in the Sichuan Basin and surrounding areas on the b_3 and b_5 surfaces of FFD, and expand into the southern MLRYR region on the b_7 and b_9

surfaces of FFD.

Figure 7 shows that the linear trend gradients b_t for LFD basically decrease from south to north as latitude increases. The linear trend gradients b_t for FFD are negatives in most part of the agricultural regions and as positives mainly in the SW and MLRYR regions, indicating a general trend of earlier arrival of LFD for most part of China from 1951 to 2012. The linear trend gradients b_t for LFD fall between -0.25 and 0 for over 54% of China most of the times. The areas associated with linear trend gradients of $-0.25 < b_t < 0$ change on different b_t surfaces of LFD. From b_3 to b_5 , the area increased markedly in QT and GX regions but decreased noticeably in the SW and MLRYR regions. From b_5 to b_7 , the area decreased in the GX region but expanded in the southern QT region. And from b_7 to b_9 , the area became relatively stabilised in most part of China, with some increase for both LP and HHH regions. Changes in the area associated with linear trend gradients of $-0.5 < b_t < -0.25$ are directly opposite to the changing patterns described above for the area associated with linear trend gradients of $-0.25 < b_t < 0$. In general, as the size of moving average window increased from 3-year through 5-year and 7-year to 9-year, areas associated with linear trend gradients of $b_t > 0$ expand, but areas associated with linear trend gradients of $b_t < -0.5$ occur only as small patches on all b_t surfaces of LFD.

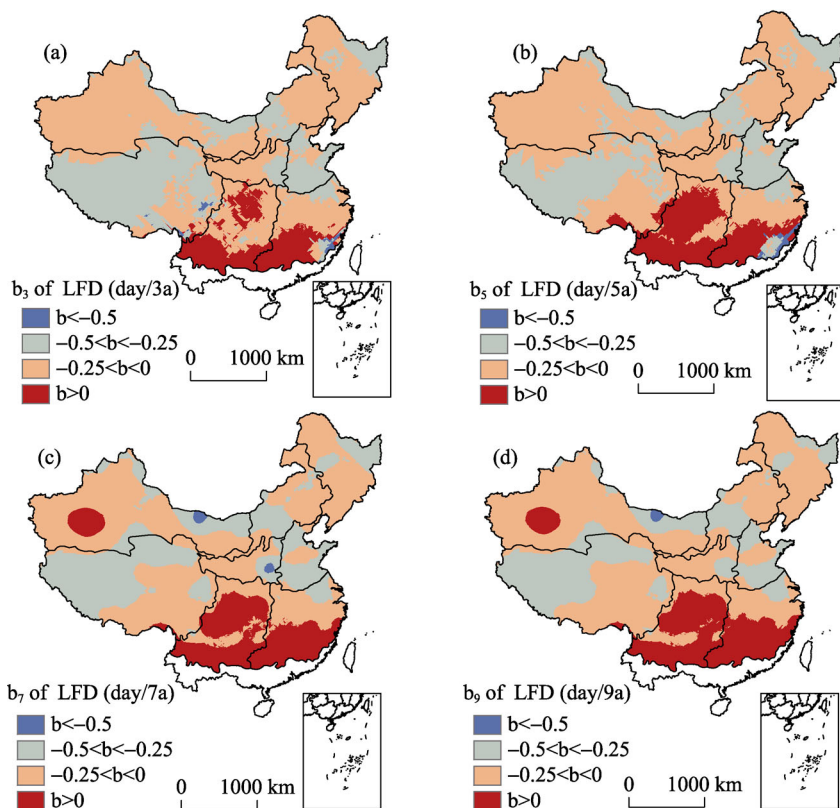


Figure 7 Surfaces of linear trend gradients b_t in LFD for the 3-, 5-, 7-, and 9-year moving averages (a, b, c, d)

Figure 8 shows that the linear trend gradients b_t for FFP are positives for over 98% of China, and areas associated with linear trend gradients of $0.25 < b_t < 0.5$ take the largest part.

Areas associated with negative linear trend gradients of $b_t < 0$ are scattered throughout the agricultural regions, with larger patches of such area concentrated mainly in the southern GX region. As the size of moving average window increased successively from 3-year through 5-year and 7-year to 9-year, the number of small patches associated with linear trend gradients of $b_t < 0$ increases, resulting in the gradual fragmentation of areas associated with linear trend gradients of $0.25 < b_t < 0.5$, and areas associated with linear trend gradients of $0 < b_t < 0.25$ expand in the LP and SW regions but show little change in the east and north ends of the NE region.

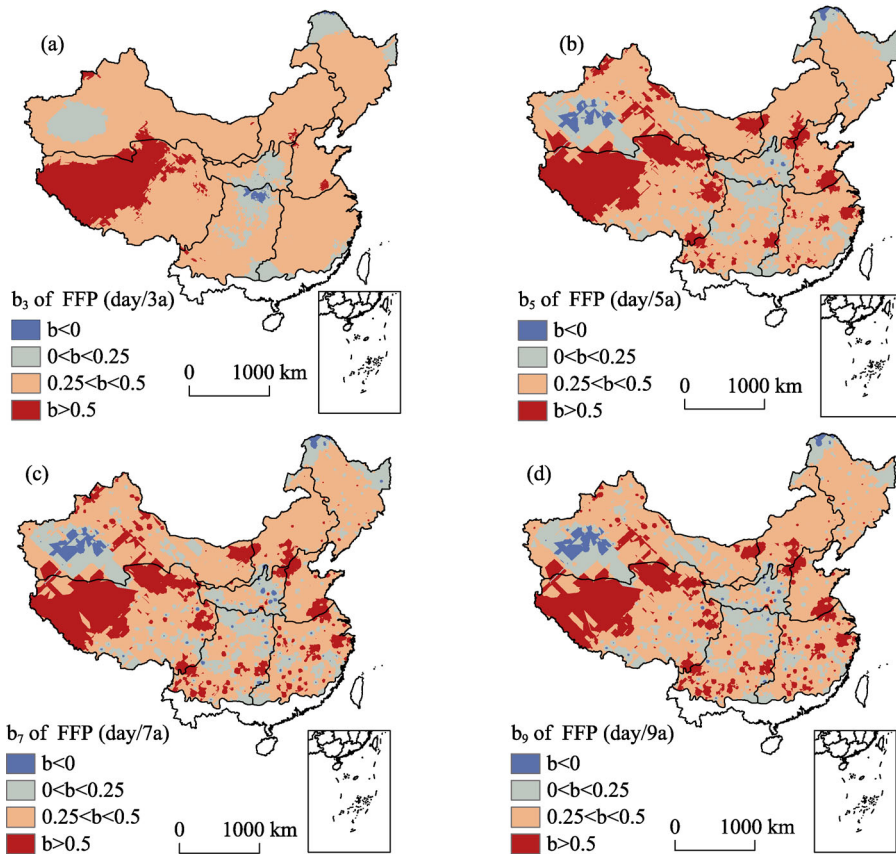


Figure 8 Surfaces of linear trend gradients b_t in FFP for the 3-, 5-, 7-, and 9-year moving averages (a, b, c, d)

Table 2 presents a summary of area percentage associated with different linear trend gradients b_t for FFD, LFD and FFP, as shown in Figures 5–7. It is clear that the 7-year moving average yields consistently the minimum percentage for the respective dominant types of areas for FFD ($0 < b < 0.25$), LFD ($-0.25 < b < 0$) and FFP ($0.25 < b < 0.5$). Accordingly, the linear trend gradients b_7 for FFD, LFD and FFP (Figures 6c, 7c, 8c) are used to further analyse the changes of their distributions throughout the agricultural regions, as well as their interrelationships.

According to the linear trend gradients b_7 for FFD, LFD and FFP (as shown in Figures 6c, 7c and 8c, and summarised in Table 3), most of the northern agricultural regions (i.e. NE, IMGWC, LP, and HHH), GX, and QT region exhibit the general trends of later FFD, earlier LFD, and extended FFP, but with some areal differentiations. For example, during the period

under consideration, in the northern QT region, FFD is 0.25–0.5 days later every 7 years, LFD is 0.25–0.5 days earlier every 7 years, resulting in a 0.5 days increase of FFP every 7 years; while in the southern QT region, FFD is 0–0.25 days later every 7 years, LFD is 0–0.25 days earlier every 7 years, resulting in 0.25–0.5 days increase of FFP every 7 years. In the southern Xinjiang part of the GX region, and in the northern part of the NE region, there exist some localised patches that have an earlier FFD, later LFD, and shortened FFP. Varying degrees of later FFD and LFD result in extended FFP across both the Sichuan Basin in the SW region and southern part of the MLRYR region. In other parts of the SW and the MLRYR regions, the FFP extended due to varying degrees of earlier FFD and LFD. In summary, the joint effects of later FFD and earlier LFD result in extended FFP in most parts of China, but for some part of China the slightly increased FFP are due to varying degrees of either earlier FFD and LFD, or later FFD and LFD.

Table 2 Distribution of area percentage associated with different linear trend gradients b_t for FFD, LFD and FFP, as shown in Figures 6–8

FFD					LFD				FFP			
	$b_t > 0$	$0 < b_t < 0.25$	$0.25 < b_t < 0.5$	$b_t > 0.5$	$b_t > -0.5$	$-0.5 < b_t < -0.25$	$-0.2 < b_t < 0$	$b_t > 0$	$b_t > 0$	$0 < b_t < 0.25$	$0.25 < b_t < 0.5$	$b_t > 0.5$
b_3	13.04	78.22	7.02	1.72	0.41	33.69	56.42	9.49	0.40	11.03	75.64	12.92
b_5	13.04	79.79	5.14	2.03	0.47	29.03	57.55	12.94	0.59	16.13	62.94	19.33
b_7	11.69	70.43	14.55	3.33	0.44	30.02	54.90	14.64	0.21	18.58	59.93	19.27
b_9	13.12	71.29	12.73	2.86	0.25	26.70	57.84	15.21	0.17	19.16	60.83	17.84

Table 3 Distribution of area percentage in different agricultural regions associated with linear trend gradients b_7 for FFD, LFD and FFP, as shown in Figures 6c, 7c and 8c

Agricultural region		FFD area percentage (%)				LFD area percentage (%)				FFP area percentage (%)			
ID (m)	Code	$b_7 > 0$	$0 < b_7 < 0.25$	$0.25 < b_7 < 0.5$	$b_7 > 0.5$	$b_7 > -0.5$	$-0.5 < b_7 < -0.25$	$-0.25 < b_7 < 0$	$b_7 > 0$	$b_7 > 0$	$0 < b_7 < 0.25$	$0.25 < b_7 < 0.5$	$b_7 > 0.5$
1	QT	4.13	90.72	5.15	0.00	0.00	55.5	43.42	1.08	4.89	45.25	43.47	6.39
2	NE	6.32	93.33	0.35	0.00	0.00	24.26	75.74	0.00	2.38	25.15	72.01	0.46
3	IMGWC	2.11	81.73	16.10	0.06	0.00	31.65	68.35	0.00	6.06	21.13	60.28	12.53
4	GX	1.08	91.99	6.93	0.00	1.10	20.71	71.26	6.93	0.00	4.87	75.63	19.50
5	LP	3.64	67.25	28.74	0.37	3.70	27.24	69.06	0.00	0.25	8.91	44.12	46.72
6	HHH	0.70	97.08	2.22	0.00	0.00	73.38	26.62	0.00	0.21	6.18	86.10	7.51
7	MLRYR	37.63	29.01	14.88	18.48	0.00	9.24	43.55	47.21	1.04	33.01	54.96	10.99
8	SW	48.01	31.89	9.20	10.90	0.00	0.38	31.38	68.24	0.38	19.28	66.97	13.37
	China	11.69	70.43	14.55	3.33	0.44	30.02	54.90	14.64	2.21	18.58	59.93	19.28

3.3.2 Spatial distribution of stations with abrupt changes in FFP

Results of Mann-Kendall tests show that intersect points between the UF_k and UB_k curves are found for all the 659 stations considered in the study, with 341 type 1 stations, 27 type 2 stations, and 291 type 3 stations (Figure 9a). It can be seen that types 1 and 3 stations are found next to each other, widely distributed, with some localised clustering; and that type 2 stations are found mainly in mountainous locations.

Geomorphologically, type 1 stations are more concentrated in the Guanzhong plain in southern LP region, the contiguous expanse of the central-southern HHH region and the northern MLRYR region, the northern HHH region, the neighbourhood of the IMGWC region, and the zones flanking the Tianshan Mountains of the GX region. Type 3 stations are more concentrated in the SW region and the neighbourhood of the MLRYR region. Statistically, as shown in Table 4, over 50% of stations in the HHH, IMGWC, NE, LP and GX regions are type 1 stations, and in the QT, MLRYR and SW regions, the percentage of all type 1 stations exceeds 40%. Over 50% of stations in the MLRYR and SW regions are type 3 stations; the percentage of type 3 stations falls between 35%–45%, in other agricultural regions except the HHH region which has the lowest percentage (28%) of type 3 stations. Figure 9b and Table 4 show that: (1) abrupt changes in FFP occurred in 46 years between

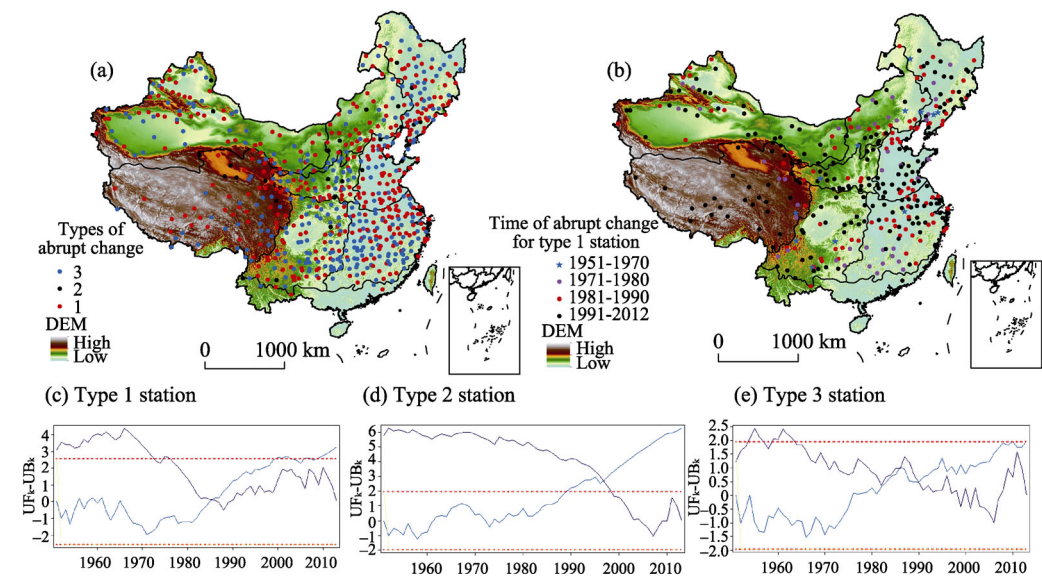


Figure 9 Spatial distribution of stations by types (a) and spatial distribution of type 1 stations by specified time (b). For type 1 stations, the UF_k and UB_k curves have only one intersect point within the confidence region ($u_{\alpha=0.05}=\pm 1.96$) (c Station ID: 56182). Type 2 stations also have only one intersect point but outside the confidence region (d Station ID: 53463). Type 3 stations have more than one intersect points (e Station ID: 50936).

Table 4 Region-based statistical summary (counts and percentages) of stations by types and by time periods

Agricultural region		Station (count)				Type 1 station (count)			
ID (k)	Code	Type 1	Type 2	Type 3	Sum	1951–1970	1971–1980	1981–1990	1991–2012
1	QT	35	6	30	71	1	5	2	27
2	NE	51	5	34	90	4	5	17	25
3	IMGWC	33	4	20	57	1	6	12	14
4	GX	45	3	39	87	0	5	12	28
5	LP	27	2	20	49	2	0	5	20
6	HHH	39	3	16	58	0	5	11	23
7	MLRYR	65	0	73	138	1	9	25	30
8	SW	45	3	58	106	3	5	12	25
9	SC	1	1	1	3	0	0	0	1
China		341	27	291	659	12	40	96	193

1951 and 2012 at the 341 type 1 stations; (2) fewer stations have abrupt changes in FFP between 1951 and 1970; (3) the number of stations with abrupt changes in FFP increased steadily since 1978, adding more than 5 stations annually; and (4) the number of stations with abrupt changes in FFP peaked in 1994.

Figure 9b and Table 4 also show that: (1) during 1951–1970, only about a dozen of stations with abrupt changes in FFP are found scattered across China; (2) during 1971–1980, a total of 40 stations with abrupt changes in FFP are found scattered in all agricultural regions, except the LP and SC regions, with the MLRYR region has the most (9 stations); (3) during 1981–1990, the number of stations with abrupt changes in FFP increased to 96, with the MLRYR region has the most (25 stations) and the QT region has the least (2 stations); and (4) during 1991–2012, the number of stations with abrupt changes in FFP reached the highest (196 stations) with the MLRYR region still has the most (30 stations); and the SC region appeared at the only type 1 station. These stations for abrupt change occurrence are concentrated in a zone extending from neighbourhood regions of the Huaihe catchment in the east, via the LP region, to the GX region in the west.

4 Discussion

This study investigated both the region-based and station-based spatial distributions of FFD, LFD and FFP across China, their temporal trends and interrelationships, with findings useful for guiding region-based management of agricultural production. During the 62-year period (1951–2012), the northern agricultural regions have witnessed steadily later FFD in autumns, earlier LFD in springs, and increasing FFP. These regions also exhibit small magnitude of inter-annual fluctuations in FFD and LFD, and accelerated increase of FFP since 1980.

The findings suggest that earlier dates of crop planting should be adopted in the NE and IMGWC regions, either to increase crop growing period or to reduce likely frost damage on crops at the final stage of growth in early autumn. Many winter varieties of wheat crops are planted over large areas in the HHH region. In early spring, post-jointing winter wheat crops are very susceptible to frost damage. Earlier LFD may reduce this susceptibility, but it is also closely linked with the rise in temperature. Warming trend in climate leads earlier jointing of wheat crops, which are very susceptible to frost damage during cold spells in early spring (Gu *et al.*, 2012; Li *et al.*, 2005).

Changes in FFD, LFD and FFP in most of the LP region are favouring crops with long growing period, increasing the yield or improving the quality of agricultural products. In the GX and QT regions, changes in FFD, LFD and FFP have little impact on agricultural productions that are dominated by animal husbandry. In oasis in the GX region and in the highland barley and rapeseed growing areas above 3800 m in altitude in the QT region, however, crop growing periods are defined by the LFD in spring and FFD in autumn. Later LFD and earlier FFD will increase crop growing period, reduce crops susceptibility to frost damage, increase the percentage of mature grains, and help winter wheat in the river valleys to live safely through the winter.

In the southern agricultural regions, the increase of FFP in different areas may result from three different mechanisms: the synergistic impact of later FFD and earlier LFD, much later FFD than LFD, and much earlier LFD than FFD. The increased FFP and associated increase in heat resources can be used to adjust the spatial arrangement of crop growing, e.g. pushing

the boundary of some crops toward the north, or adopting crop varieties with longer growing periods. We should pay attention to possible meteorological hazards due to the irregular occurrence of frost when FFP exhibits a trend of increase. For example, during periods of higher dekad (ten days) or monthly mean temperatures, 3 consecutive daily minimum temperatures lower than 5°C could result in cold damage in the southern regions, let alone the occurrence of frosts when daily minimum temperatures are lower than 0°C. Therefore, we should be prudent when making such adjustments in crop growth in southern agricultural regions to minimize the negative impact of meteorological hazards.

Some aspects of the study have been identified for improvement in future studies. First, the dataset used in the study should be improved. This study is based on daily minimum temperature recorded at 823 meteorological stations across China. We identified stations with incomplete records for the 62 years and excluded them from further analysis. We calculated FFD, LFD and FFP for each of the remaining stations, converted the FFD and LFD into Julian dates, and analysed their changing trends. The direct exclusion of stations with incomplete records is not desirable since it reduced the density of data points in space. One way to improve is to estimate the missing records using neighbouring observations in space and/or time. The use of Julian calendar for dates of FFD and LFD can result in incorrect FFP values and pseudo changing trends, especially in the southern agricultural regions. The dates for FFD and LFD in the southern agricultural regions may fluctuate between December and January. When transformed using the Julian dates, shorter interval between actual dates of FFD and LFD may appear much longer, affecting the outcome of analysis. One way to reduce this effect is to use, for example, day one in the warmest or coldest month as the first day of the year in transforming dates for FFD and LFD.

Second, the characterisation of changes in FFD, LFD and FFP may be improved. In this study, a few key time snapshots are used to analyse the changing spatial distribution of FFP across China. In the future, we may overlay annual spatial distributions to identify and delineate both core areas where climate conditions are relatively stable over time and peripheral zones where climate conditions exhibit more pronounced fluctuations. We probably should pay more attention to these more dynamic peripheral zones when studying agricultural adaptation under changing climate. In addition, changes of climate variables over time (e.g. during the 62 years considered in this study) may well be non-linear, with some periodic or rhythmic fluctuations. In this study, we used moving average smoothing to minimise the impact of extreme climate events, and the linear fitting technique adopted is inadequate for uncovering more characteristics of changes in FFD, LFD and FFP. Finally, Geomorphology imposes obvious influence on regional changes of climate variables. This study only applied simple overlay of station-based changes in FFP with a DEM. Clearly, geomorphological influence on the distributions and changes in FFD, LFD and FFP deserve more in depth analysis in the future.

5 Conclusions

This study examined daily minimum temperatures for 823 national-level meteorological stations and determined annual station-specific dates of FFD and LFD, and lengths of FFP from 1951 to 2012, computed region-specific values of FFD, LFD and FFP, including the annual regional averages and cumulative deviations from the means, for the 9 agricultural

regions; estimated the gradients of linear regression for station-specific 3-, 5-, 7-, and 9-year moving averages of FFD, LFD and FFP, and mapped their spatial variations across China; assessed station-specific time series of FFP and detected times of abrupt changes.

The results revealed the following characteristics of the spatio-temporal variations in FFD, LFD and FFP:

(1) In general, at both the station level and the regional level, the FFP across China decreases with the increase of latitude from south to north, and with the increase of altitude from east to west.

(2) The station-level standard deviations of FFD, LFD and FFP decrease with the increase of latitude from south to north, but increase with the increase of altitude from east to west, indicating the inter-annual fluctuations in FFD, LFD and FFP in the south and west agricultural regions are greater than that in the north and east agricultural regions.

(3) At the regional level, temporal changes in the length of FFP from 1951 to 2012, as indicated by the CDFM curves are relatively small in both the low latitude region (SC) and the high latitude regions (GX and NE), but for the mid-latitude regions (IMGWC, LP, HHH, MLRYR, and SW), the length of FFP decreases till the 1980s and then increases. Influenced by high altitudes, the QT region shows a unique pattern of changes in the length of FFP, increases till the 1960s, then decreases till the 1980s, and then increases again.

(4) In general, over 80% of China exhibits a later FFD and earlier LFD, and consequently, increased FFP. However, there exist some regional differences. For instance, in the north and east regions, temporal variations in FFD, LFD and FFP exhibit higher magnitudes than that in the southern and western agricultural regions. In many agricultural regions, NE, GX, IMGWC, LP, HHH, and some areas in the SW and MLRYR regions, the increase in FFP is due to the later FFD and earlier LFD. But for other areas in the SW and MLRYR regions, the increase in FFP is resulted either from much delayed FFD and slightly delayed LFD, or from slightly earlier FFD and much earlier LFD.

(5) Among the 659 station-specific time series of FFP examined with the Mann-Kendall test, 341 stations (52%), located mainly in the IMGWC, HHH, QT, and GX regions, and the central-western part of the NE, have one identifiable and significant abrupt change detected. And at the 341 stations with identified abrupt changes, most (57%) abrupt changes occurred during 1991–2012, followed by the periods of 1981–1990 (28%) and 1971–1980 (12%), and less than 4% occurred during 1951–1970.

(6) The improved understanding on the characteristic spatio-temporal variations of FFD, LFD and FFP, achieved through this study, would provide important guidance to regional agricultural practices. The increased FFP may help to extend crop growing period, increase crop yield, improve agricultural products quality, and reduce crops susceptibility to frost damage in NE, IMGWC and LP regions, in the oasis of GX region and the highland barley growing areas in QT region. For the HHH region, earlier arrival of LFD may help to reduce the susceptibility of winter wheat crops to frost damage, but the warming trend in climate change may lead to earlier jointing of wheat crops, which can be very susceptible to frost damage during cold spells in early spring. In the southern regions, possible meteorological hazards may result from the irregular occurrence of frost even with the increase trend of FFP.

References

- Bai Q F, Li X M, Zhu L, 2013. The changes of the frost-free periods from 1961 to 2010 and its impact on apple industry in Shanxi province. *Journal of Arid Land Resources and Environment*, 27(8): 65–70. (in Chinese)
- Chen S Y, Zhang Y X, Lou W P *et al.*, 2013. Changes in the first frost date from 1961 to 2009 in Northwest China. *Resources Science*, 35(1): 165–172. (in Chinese)
- Dai J H, Wang H J, Ge Q S, 2013. Changes of spring frost risks during the flowering period of woody plants in temperate monsoon area of China over the past 50 years. *Acta Geographica Sinica*, 68(5): 593–601. (in Chinese)
- Du J, Shi L, Yuan L, 2013. Responses of climatic change on the frost days in main agricultural area of Tibet from 1961 to 2010. *Chinese Journal of Agrometeorology*, 34(3): 264–271. (in Chinese)
- Du L, Zhao G X, Yang L M, 2014. The variation characteristics analysis of frost in Chongqing City in recent 40 years. *Chinese Agricultural Science Bulletin*, 30(17): 279–283. (in Chinese)
- Edmar I T, Guenther F, Harrij V V *et al.*, 2013. Global hot-spots of heat stress on agricultural crops due to climate change. *Agriculture and Forest Meteorology*, 170: 206–215.
- Editorial Committee of the National Agricultural Zoning Committee ‘Comprehensive Agricultural Regionalization in China’ (NAZC), 1981. Comprehensive Agricultural Regionalization in China. Beijing: Agricultural Press. (in Chinese)
- Fu C B, Wang Q, 1992. The definition and detection of the abrupt climatic change. *Scientia Atmospherica Sinica*, 16(4): 482–493. (in Chinese)
- Goossens C, Berger A. 1986. Annual and seasonal climatic variations over the Northern Hemisphere and Europe during the last century. *Annales Geophysicae*, 4(4): 385–400.
- Gu W L, Ji X J, Zhu Y Y *et al.*, 2012. Risk regionalization of winter wheat late freezing injury in Henan province. *Journal of Catastrophology*, 27(3): 39–44. (in Chinese)
- Han R Q, Li W J, Ai W X *et al.*, 2010. The climatic variability and influence of first frost dates in Northern China. *Acta Geographica Sinica*, 65(5): 525–532. (in Chinese)
- Hu Q, Pan X B, Zhang D, 2015. Variation of temperature and frost-free period in different time scales in Northeast China. *Chinese Journal of Agrometeorology*, 36(1): 1–8. (in Chinese)
- IPCC, 2014. Climate Change 2014: Impact, Adaptation and Vulnerability [M/OL]. Cambridge: Cambridge University Press (in press). <http://www.ipcc-wg2.gov/>.
- Kendall M A, Stuart A, 1967. The Advanced Theory of Statistics. 2nd ed. Londres: Charles Griffin.
- Labaciren, Suolangjiacuo, Baima, 2014. Spatial and temporal distribution of frost days over Tibet from 1981 to 2010. *Acta Geographica Sinica*, 69(5): 690–696. (in Chinese)
- Li F, Zhang J X, Wu Y L *et al.*, 2013. Spatial and temporal distribution and its impact factors of the last frost over Shanxi Province from 1961 to 2010. *Acta Geographica Sinica*, 68(11): 1472–1480. (in Chinese)
- Li M S, Wang D L, Zhong X L *et al.*, 2005. Current situation and prospect of research on frost of winter wheat. *Journal of Natural Disasters*, 14(4): 72–78. (in Chinese)
- Li S, Shen Y J, 2013. Impact of climate warming on temperature and heat resource in arid Northwest China. *Chinese Journal of Eco-Agriculture*, 21(2): 227–235. (in Chinese)
- Li S K, Hou G L, Ouyang Hai *et al.*, 1988. Agricultural Climate Resources and Agricultural Climate Zoning of China. Beijing: Science Press. (in Chinese)
- Mann, H. B. 1945. Non-parametric tests against trend. *Econometrica*, 3(13): 245–259.
- Pan S K, Zhang M J, Wang B L *et al.*, 2013 Changes of the first frost dates, last frost dates and duration of frost-free season in Xinjiang during the period of 1960–2011. *Arid Zone Research*, 30(4): 735–742. (in Chinese)
- Qian B D, Gameda S, Zhang X B *et al.*, 2012. Changing growing season observed in Canada. *Climatic Change*, 112: 339–353.
- Qian J X, Zhang X, Zhang J X *et al.*, 2010. The changing trends of the first and last frost dates over Shanxi prov-

- ince for the past 40 years. *Acta Geographica Sinica*, 65(7): 802–808. (in Chinese)
- Ramirez-Villegas J, Jarvis A, Läderach P, 2013. Empirical approaches for assessing impacts of climate change on agriculture: The EcoCrop model and a case study with grain sorghum. *Agricultural and Forest Meteorology*, 170: 67–78.
- Skaggs K E, Irmak S, 2012. Long-term trends in air temperature distribution and extremes, growing degree-days, and spring and fall frosts for climate impact assessments on agricultural practices in Nebraska. *Journal of Applied Meteorology and Climatology*, 51(11): 2060–2073.
- Tang G A, Yang X, 2012. ArcGIS: GIS Spatial Analysis Experiment Tutorial. Beijing: Science Press. (in Chinese)
- Wang B Y, Fan G Z, Wei M *et al.*, 2014. Frost spatial and temporal variations analysis in Hengduan Mountains. *Plateau and Mountain Meteorology Research*, 34(2): 17–21. (in Chinese)
- Wei F Y, 2007. Modern Climate Statistics Diagnosis and Prediction Technology. 2nd ed. Beijing: China Meteorological Press. (in Chinese)
- Xu J H, 2012. Mathematical Methods in Contemporary Geography. Beijing: Higher Education Press. (in Chinese)
- Ye D X, Zhang Y, 2008. Characteristics of frost changes from 1961 to 2007 over China. *Journal of Applied Meteorological Science*, 19(6): 661–665. (in Chinese)
- Zhang D, Xu W H, Li J Y *et al.*, 2014. Frost-free season lengthening and its potential cause in the Tibetan Plateau from 1960 to 2010. *Theoretical and Applied Climatology*, 115(3/4): 441–450.
- Zhang L, Zhang X Y, Li H Y *et al.*, 2013. Characteristics of frost-free days changes over Ningxia from 1961 to 2010. *Ecology and Environmental Sciences*, 22(5): 801–805. (in Chinese)
- Zhang S Q, Pu Z C, Li J L *et al.*, 2013. The impact of global warming on frost-free periods from 1961 to 2010 in Xinjiang. *Resources Science*, 35(9): 1908–1916. (in Chinese)